

## DISCOVERY OF AN OBSCURED BROAD LINE REGION IN THE HIGH REDSHIFT RADIO GALAXY MRC 2025-218

JAMES E. LARKIN<sup>1</sup>, IAN S. MCLEAN<sup>1</sup>, JAMES R. GRAHAM<sup>2</sup>, E. E. BECKLIN<sup>1</sup>, DONALD F. FIGER<sup>3</sup>,  
ANDREA M. GILBERT<sup>2</sup>, N. A. LEVENSON<sup>2,4</sup>, HARRY I. TEPLITZ<sup>5,6</sup>, MAVOURNEEN K. WILCOX<sup>1</sup> &  
TIFFANY M. GLASSMAN<sup>1</sup>

<sup>1</sup>Dept. of Physics and Astronomy, University of California, Los Angeles, <sup>2</sup>Dept. of Astronomy, University of California, Berkeley, <sup>3</sup>Space Telescope Science Institute, <sup>4</sup>Dept. of Physics and Astronomy, John's Hopkins University, <sup>5</sup>LASP, Goddard Space Flight Center, <sup>6</sup>NOAO Research Associate

*Draft version October 29, 2018*

### ABSTRACT

This paper presents infrared spectra taken with the newly commissioned NIRSPEC spectrograph on the Keck II Telescope of the High Redshift Radio Galaxy MRC 2025-218 ( $z=2.63$ ). These observations represent the deepest infrared spectra of a radio galaxy to date and have allowed for the detection of H $\beta$ , [OIII] (4959/5007), [OI] (6300), H $\alpha$ , [NII] (6548/6583) and [SII] (6716/6713). The H $\alpha$  emission is very broad (FWHM = 9300 km/s) and luminous ( $2.6 \times 10^{44}$  ergs/s) and it is very comparable to the line widths and strengths of radio loud quasars at the same redshift. This strongly supports AGN unification models linking radio galaxies and quasars, although we discuss some of the outstanding differences. The [OIII] (5007) line is extremely strong and has extended emission with large relative velocities to the nucleus. We also derive that if the extended emission is due to star formation, each knot has a star formation rate comparable to a Lyman Break Galaxy at the same redshift.

*Subject headings:* galaxies: active — galaxies: structure — galaxies: quasars — galaxies: kinematics and dynamics — infrared: galaxies

### 1. INTRODUCTION

Deep radio surveys have proven to be one of the best methods for finding high redshift galaxies. Most evidence suggests that these powerful radio sources are the precursors of local giant ellipticals (e.g. Pentericci, et al. 1999). Many have irregular and complex morphologies suggestive of mergers and they are often surrounded by an overdensity of compact sources; presumably sub-galactic clumps (e.g. van Breugel et al. 1998). At both low and high redshifts, radio galaxies usually have strong optical emission lines, especially OIII at 5007 Å. It is strongly debated, however, if the emission lines arise by the same mechanism as the radio jets. Several authors (e.g. Rawlings & Saunders 1992, Eales & Rawlings 1993, and Evans 1998) have demonstrated a strong correlation between radio luminosity and [OIII] luminosity, but as Evans showed, there is a strong selection effect based on the detection limits as a function of distance and this may explain much of the correlation. Since the galaxies are often disturbed, star formation, large scale shocks and a central AGN are all possible sources of the line emission. Active galaxy unification models suggest that radio galaxies are quasars with obscured broad line regions (e.g. Antonucci 1993). Eales & Rawlings (1993, 1996) and Evans (1998) have been successful at using infrared spectrographs on 4-meter class telescopes to measure a few of the brightest lines in small samples of radio galaxies in the redshift range 2.2 to 2.6 and they find line ratios most consistent with Seyfert 2 (obscured AGN) nuclei. Independent of our current efforts, a team has also successfully used the ISAAC instrument on the VLT to observe high redshift radio galaxies (HzRGs) including MRC 2025-218 (McCarthy, personal communication).

An additional unexplained phenomenon is that at high

redshifts ( $z>0.6$ ) the radio, optical continuum, infrared continuum and emission line structures tend to be closely aligned (Chambers, Miley, & van Breugel 1987, and McCarthy et al. 1987). This is probably not seen in lower redshift targets because the central activity tends to be a smaller fraction of the total luminosity than in high redshift sources. Among the proposed explanations are that the emission lines arise from shock induced star formation (De Young 1989, Rees 1989) or that it is scattered light originating from the central nucleus (Fabian 1991). This is a crucial question in our understanding of how and when most star formation occurred in giant elliptical galaxies and in clusters in general.

MRC 2025-218 ( $z=2.630$ ) has a compact near infrared and optical continuum morphology (van Breugel et al. 1998), but extended Ly $\alpha$  emission (5'') aligned with its radio axis (McCarthy et al. 1992). The extended UV emission has significant ( $8.3 \pm 2.3$  %) linear polarization perpendicular to the UV axis (Cimatti et al. 1996) suggesting that scattering plays a significant role. McCarthy et al. also found three extremely red galaxies (ERO's:  $R-K > 6$  mag) within 20'' of the radio galaxy. This is a large overdensity of such objects and strongly suggests an association between the ERO's and the active galaxy. In this paper we present infrared spectra taken with a long slit oriented close to the radio axis and including one of the ERO's. The ERO spectra will be described in a future paper. For all calculations we have assumed a cosmology with  $\Lambda=0$ ,  $q_0=0.1$  and  $H_0=75$  km s<sup>-1</sup> Mpc<sup>-1</sup>. For a redshift of 2.63 this yields a luminosity distance of  $2.1 \times 10^4$  Mpc and an angular scale of 7.7 kpc per arcsecond.

### 2. OBSERVATIONS AND DATA REDUCTION

The field of MRC 2025-218 was observed on 4 Jun, 1999 (UT) with the near infrared spectrograph NIRSPEC

(McLean, et al. 1998 and McLean, et al. 2000) on the Keck II Telescope during its commissioning. First the field was imaged in the K-band with the slitviewing camera which is a HgCdTe PICNIC detector ( $256^2$  pixels) sensitive from 1 to 2.5 microns. Figure 1 shows the reduced image of the field with a total integration time of 540 seconds and a FWHM of  $0''.54$ . As shown in the figure, the slit ( $42''$  long and  $0''.57$  wide) was placed on both the radio galaxy and the extremely red galaxy dubbed ERO-A by McCarthy et al. (1992). This corresponded to a slit position angle of  $-7$  degrees.

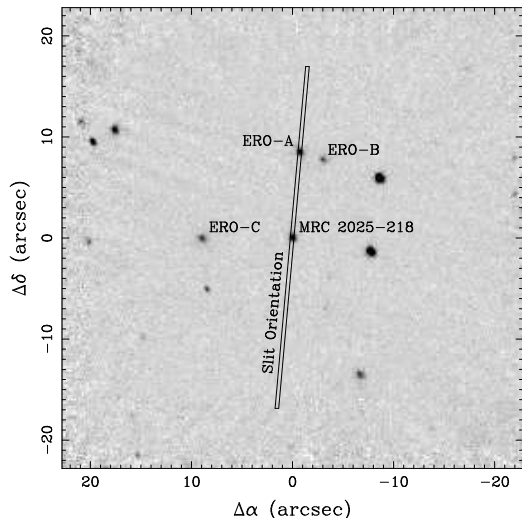


Figure 1. - K band image of the MRC 2025-218 field.

For spectroscopy, the telescope was repeatedly moved roughly 20 arcseconds to center the objects first in the upper portion of the slit then the lower portion. Four 300 second exposures were taken in both the H-band ( $\sim 1.6\mu\text{m}$ ) and K-band ( $\sim 2.2\mu\text{m}$ ) yielding an effective integration time on MRC 2025-215 of 20 minutes in each band. For guiding, NIRSPEC's optical guide camera was used to actively track a bright star roughly 2 arcminutes from MRC 2025-218.

Arc lamp and flat lamp spectra were taken at each setting prior to changing mechanism setups. The 7.6 magnitude A0 star PPM 272233 was also observed at the same settings in order to remove telluric absorption effects from the atmosphere. The calibrator star was reduced first. For each band the spectral pair was subtracted and divided by a reduced flat field lamp spectra. Bad pixels were then identified and removed by medianing the four nearest neighbors. The spectra were spatially rectified using a quadratic polynomial at each row, then spectrally rectified with a quadratic at each column. The negative spectrum of the star was then shifted and subtracted from the positive spectrum producing a combined spectrum with residual atmospheric lines removed. The stellar spectrum was extracted by averaging the central 3 pixels along the 2-d spectrum. A synthetic black body spectrum was divided into the stellar spectrum and residual hydrogen absorption lines from the Brackett series were interpolated over. The spectra of the radio galaxy were reduced in a similar way except they were divided by the reduced calibration star spectrum instead of a black body. For extraction of the galaxy spectra, a 6 pixel spatial aperture ( $1''.14$ ) was used. Spectrophotometry was obtained by determining

the equivalent widths of the emission lines within a  $1''.5$  aperture in the spectra and comparing this to the broad band fluxes of the galaxy in a  $1''.5$  circular aperture in the slit viewing camera images.

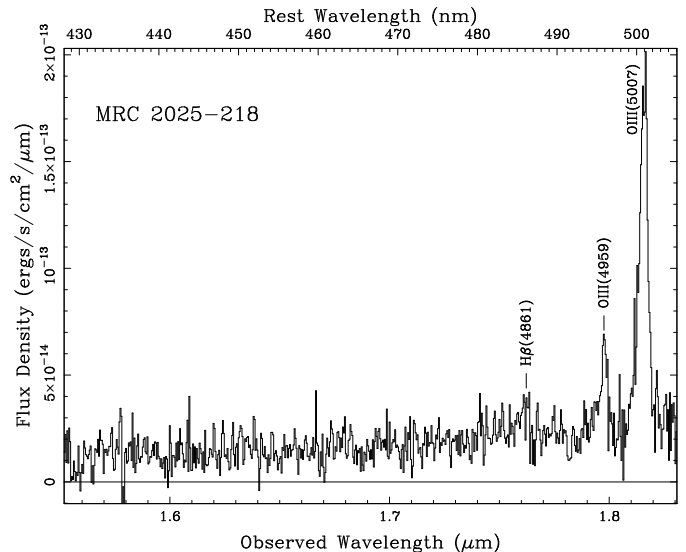


Figure 2. - H band spectrum of MRC 2025-218. It is dominated by [OIII] at rest wavelength 5007 Å. Also present is the other member of this doublet ([OIII], 4959 Å) and a weak H $\beta$  emission line.

### 3. RESULTS

Figure 2 shows the H-band spectrum of MRC 2025-218. By far the most dominant line is [OIII] (5007 Å) redshifted to  $1.82\mu\text{m}$ . This line is highlighted in figure 3 where the complete position velocity map of this line is presented. Panel (a) of figure 3 is stretched to highlight the spectrally double nature of the nuclear emission ( $\Delta v \sim 200\text{ km sec}^{-1}$ ). Panel (b) shows three faint emission knots at large angular separations ( $1''$ - $2''$ ) and/or high kinematic velocities ( $\sim 400\text{ km s}^{-1}$ ) Although faint, these structures repeat in the individual spectra that cover the [OIII] line. Two knots appear at essentially  $0\text{ km sec}^{-1}$  relative velocity, but  $1''.8$  North and  $2''.4$  South of the Nucleus. A high speed clump appears  $1''$  North of the nucleus and at a redshifted relative velocity of  $410\text{ km sec}^{-1}$ . This high speed clump is also the brightest within our slit with a flux of roughly  $1 \times 10^{-16}\text{ ergs s}^{-1}\text{ cm}^{-2}$ . Also detected in the H-band spectrum is the other member of the [OIII] doublet at 4959 Å, and H $\beta$ . The ratio of [OIII] / H $\beta$  is extremely large at  $17 \pm 7$ . The H $\beta$  line has a total nuclear flux of only  $5 \times 10^{-17}\text{ ergs cm}^{-2}\text{ s}^{-1}$ . Table 1 gives all detected fluxes and line widths.

Figure 4 shows the K-band spectrum which is dominated by a broad H $\alpha$  emission line. The spectrum has had a median filter passed over it to improve the appearance of the fainter lines. The H $\alpha$  is well modeled by a pair of Gaussians having line widths of  $9300 \pm 900\text{ km/s}$  and  $730 \pm 100\text{ km/s}$ . The narrow component is consistent with the Ly $\alpha$  line width of  $700\text{ km/s}$  found by Villar-Martin et al. 1999. After subtracting away the two H $\alpha$  components, the middle graph in figure 4 shows the strong [NII] (6548/6583 Å) emission lines as well as weaker features from [OI] (6300 Å) and [SII] (6716/6731 Å). The line fluxes and widths are also given in table 1.

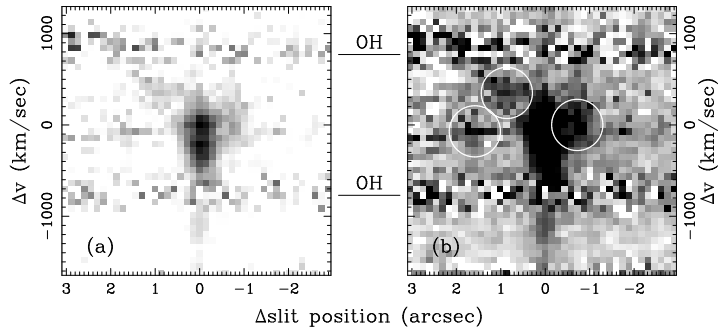


Figure 3. - Position velocity plots for OIII (5007). Panel (a) is stretched to show the double nuclear peak. Panel (b) highlights three extended emission regions circled in white. The OIII line is highly disturbed with several different kinematic and spatial components including a kinematically split nucleus and a high velocity (400 km/s) knot located 2" off nucleus. Nearby OH lines from the Earth's atmosphere are labeled.

TABLE 1  
Emission Line Strengths

Line	Rest $\lambda(\text{\AA})$	Flux ( $\times 10^{-16}$ ergs $\text{s}^{-1}$ $\text{cm}^{-2}$ )	Line Width ( $\text{km s}^{-1}$ )
SII	6731	$0.4 \pm 0.3$	$200 \pm 100$
SII	6716	$0.6 \pm 0.3$	$200 \pm 100$
NII	6583	$1.3 \pm 0.3$	$880 \pm 100$
NII	6548	$1.3 \pm 0.3$	$880 \pm 100$
H $\alpha$ (narrow)	6563	$2.7 \pm 0.4$	$730 \pm 100$
H $\alpha$ (broad)	6563	$18 \pm 2$	$9300 \pm 900$
OI	6300	$0.8 \pm 0.3$	$800 \pm 400$
OIII	5007	$8.4 \pm 1.6$	$600 \pm 200$
OIII	4959	$2.1 \pm 0.4$	$600 \pm 200$
H $\beta$	4861	$0.5 \pm 0.3$	$600 \pm 200$

## 4. DISCUSSION

### 4.1. Nuclear Spectrum

The nuclear spectrum of the HzRG MRC 2025-218 is clearly dominated by emission lines from a central AGN. The broad H $\alpha$  line width is 9300 km/s which is only seen in type I AGN (unobscured broad line regions). This line width is very close to the mean H $\beta$  line width of  $9870 \pm 950$  km/s of radio loud quasars in the redshift range 2.0 to 2.5 by McIntosh et al., 1999. The ratio of [OIII]/H $\beta$  is 17 which is also only seen in AGN and ratios of [NII]/H $\alpha$  and [OI]/H $\alpha$  are also consistent with AGN excitation (Osterbrock, 1989).

From the H $\alpha$ /H $\beta$  narrow line ratio of 5.4 we derive an optical extinction  $A_V = 1.4$  mag. In this calculation we've assumed an intrinsic ratio of H $\alpha$ /H $\beta$  = 3.1 as seen in local AGN (Osterbrock, 1989), and the interstellar extinction law of Cardelli et al. (1989). This must be treated as an upper limit, however, since radio loud objects may have elevated H $\alpha$  due to collisional excitation (e.g. Baker et al. 1994). If the broad line ratio of H $\alpha$ /H $\beta$  were similar to the narrow line ratio, then broad H $\beta$  should have marginally been detected in our H-band spectrum. We therefore feel safe in the assumption that the extinction to the broad line region is similar to the value for the narrow line region (1.4 mag), but not necessarily significantly greater. This extinction is also sufficient to explain the lack of broad Ly $\alpha$  detections in McCarthy et al. (1990) and Villar-Martin et al. (1999b). Without extinction our broad line emission would predict a Ly $\alpha$  broad line flux of

$2.6 \times 10^{-15}$  ergs  $\text{s}^{-1}$   $\text{cm}^{-2}$  in the Villar-Martin slit which would have been easily detected but with  $A_V = 1.4$  mag this is reduced to less than  $3 \times 10^{-16}$  ergs  $\text{s}^{-1}$   $\text{cm}^{-2}$  which would have been marginally detected at best.

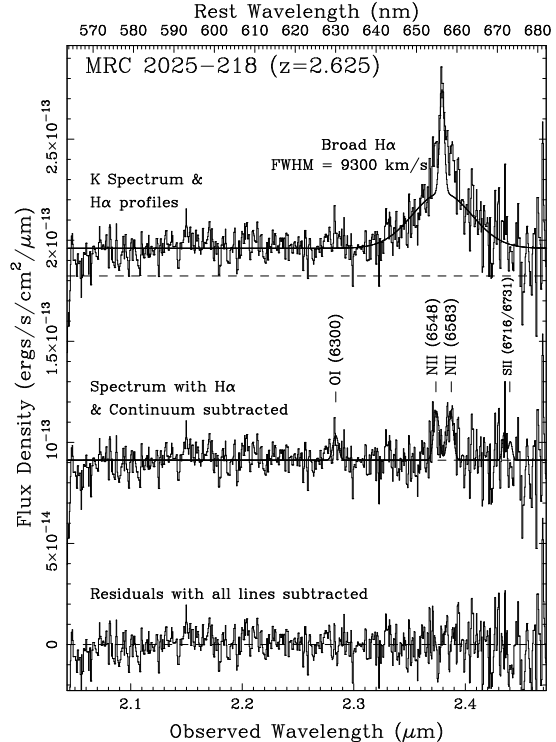


Figure 4. - The K band spectrum of MRC 2025-218 is dominated by a very wide (9300  $\text{km s}^{-1}$ ) strong emission line of H $\alpha$ . The upper graph is the reduced spectrum overlaid with the H $\alpha$  profiles. The dashed line is the x-axis for this graph. The middle graph has had the continuum and H $\alpha$  emission lines subtracted to emphasize the weaker lines of NII. The bottom graph is the residuals after subtracting Gaussians for each emission line.

Given the similarities in line width with radio loud quasars we now try to determine if the extinction could explain the observed differences between MRC 2025-218 and radio loud quasars. If we correct the H $\alpha$  flux for  $A_V = 1.4$  mag (the upper limit to the narrow line extinction), then the broad line flux becomes  $5.2 \times 10^{-15}$  ergs  $\text{s}^{-1}$   $\text{cm}^{-2}$  or a broad line H $\alpha$  luminosity of  $2.6 \times 10^{44}$  ergs  $\text{s}^{-1}$ . We used the sample of quasars of McIntosh et al. (1999) to derive a mean H $\alpha$  luminosity of  $6.11 \times 10^{44}$  ergs  $\text{s}^{-1}$  based on the mean H $\beta$  equivalent width of their sample, no extinction and an intrinsic ratio of 3.1 between H $\alpha$  and H $\beta$ . The one sigma dispersion in this value is only 10% in their sample. Our extinction corrected H $\alpha$  luminosity is then weaker than their mean by a factor of 2.6 suggesting the central engines are very similar. If we go a step further and assume that the intrinsic luminosities are the same, then the broad line extinction would need to be  $A_V = 3.5$  mag instead of  $A_V = 1.4$  mag as derived above for the narrow line region.

A remaining difference between MRC 2025-218 and the quasars in the McIntosh sample is the H-band magnitude. MRC 2025-218 has a broad band magnitude of  $H = 19.1$  while the mean quasar H-band magnitude is 15.16. After correcting for the different redshifts (quasar mean  $z = 2.2$ ) then MRC 2025-218 is 3.2 magnitudes fainter than the

quasars at a rest wavelength of 4550 Å. If the broad band flux of MRC 2025-218 is dominated by the AGN then it would require  $A_V=4.2$  mag to make it equal to the quasar sample. This is surprisingly close to the value of 3.5 mag required to match the broad  $H\alpha$  fluxes. The assumption that the AGN dominates the broad band flux in a radio galaxy, however, is not obvious and may be in conflict with the empirically determined K magnitude versus redshift relation observed in both low redshift and high redshift objects (Eales et al. 1997). MRC 2025-218 is consistent with the K vs. Z relation both with and without taking the line emission into account.

Villar-Martin et al. (1999) find that MRC 2025-218 has large ratios of  $[NV]/HeII$  and  $[NV]/[CIV]$  and suggest that the most likely explanation is that N is overabundant. They held out the possibility, however, that contamination from a broad line region was enhancing this line in comparison to their other radio galaxies. But they argued against this due to the lack of any broad lines including  $[CIII]$ . From our broad  $H\alpha$  detection, however, we clearly see that the broad line region is only partially obscured and the strong NV emission is probably not indicative of high metallicity. This is further corroborated by the relatively low ratios of  $[NII]/H\alpha(\text{narrow})$ .

#### 4.2. Spectral Shape and Extended Emission

The double spectral peak found in  $[OIII]$  could be due to a high velocity ( $200 \text{ km s}^{-1}$ ) cloud of gas or possibly a double active nucleus. The unsmoothed  $H\alpha$  narrow line is quite noisy but also shows a double profile with a separation of  $200 \text{ km s}^{-1}$ . Due to the noise, however, we are not confident in the second  $H\alpha$  peak. If the second peak were due to a star forming region it would be unlikely that the  $[OIII]$  line would be double as well since the  $OIII/H\beta$  ratio should be much lower for a starburst.

The off nucleus knots seen in  $[OIII]$  are difficult to understand. Extended  $OIII$  has been observed in other radio galaxies aligned to the radio axis (Armus et al. 1998) but no line ratios have been determined for this gas. If we assume that the emission is from starbursts then our brightest knot ( $1 \times 10^{-16} \text{ ergs s}^{-1} \text{ cm}^{-2}$ ) would have an  $[OIII]/H\alpha$  ratio less than 1.0. This would make the  $H\alpha$  flux greater than  $1 \times 10^{-16} \text{ ergs s}^{-1} \text{ cm}^{-2}$  and a luminosity more than  $5 \times 10^{42} \text{ ergs s}^{-1}$ . Assuming the relationship of Kennicutt (1983) that the star formation rate is equal to

$L(H\alpha)$  divided by  $1.12 \times 10^{41} \text{ ergs/s}$  we derive a star formation rate of  $45 M_{\odot} \text{ yr}^{-1}$ . This is comparable to the rates seen in Pettini et al. (1998) where they studied 5 star forming galaxies in the redshift range 2.2 to 3.3. This is also close to the estimated star formation rate of the Lyman Break Galaxy MS1512-cB58. As calculated in Teplitz et al. (2000) cB58 has a SFR of  $620 M_{\odot} \text{ yr}^{-1}$  but after removing a factor of 30 for gravitational lensing this becomes  $21 M_{\odot} \text{ yr}^{-1}$ .

#### 5. CONCLUSIONS

We have obtained the most sensitive infrared spectra ever taken of a high redshift radio galaxy. The galaxy has very strong emission lines with ratios and line widths consistent with an obscured quasar. The narrow line region appears to be partially obscured with  $A_V$  around 1.4 mag, but from comparisons with high redshift quasars, we estimate that the extinction to the broad line region is between 3 and 5 magnitudes. Since other radio galaxies in the same redshift range don't show broad emission lines, we suggest that MRC 2025-218 is further along in its evolution towards an unobscured quasar. We cannot rule out any of the proposed mechanisms for the production of the aligned emission. But based on the  $[OIII]$  line strength if the majority of the emission is due to star formation, we find that the star formation rate is comparable to that of Lyman Break Galaxies at similar redshifts. We urge even deeper observations of this and other similar radio galaxies in order to measure additional extended line emission.

It is a pleasure to acknowledge the hard work of past and present members of the NIRSPEC instrument team at UCLA: Maryanne Angliongto, Oddvar Bendiksen, George Brims, Leah Buchholz, John Canfield, Kim Chin, Jonah Hare, Fred Lacayanga, Samuel B. Larson, Tim Liu, Nick Magnone, Gunnar Skulason, Michael Specncer, Jason Weiss and Woon Wong. In addition, we thank the Keck Director Fred Chaffee, CARA instrument specialist Thomas A. Bida, and all the CARA staff involved in the commissioning of NIRSPEC. We also want to thank Lee Armus for many useful discussions. We are also grateful for a very careful review from our anonymous referee. Data presented herein were obtained at the W.M. Keck Observatory which was made possible by the generous financial support of the W.M. Keck Foundation.

#### REFERENCES

- Antonucci, R. 1993, *ARA&A*, 31, 473  
 Armus, L., Soifer, B. T., Murphy, T. W., Neugebauer, G., Evans, A. S., & Matthews, K. 1998, *ApJ*, 495, 276  
 Baker, A. C., Carswell, R. F., Bailey, J. A., Espey, B. R., Smith, M. G., & Ward, M. J. 1994, *MNRAS*, 270, 575 A. S., & Matthews, K. 1998, *ApJ*, 495, 276  
 Binney, J. & Tremaine, S. 1987, *Galactic Dynamics*, (Princeton: Princeton University Press  
 Cardelli, J. A., Clayton, G. C. & Mathis, J. S. 1989, *ApJ*, 345, 245  
 Chambers, K. C., Miley, G. K., van Breugel, W. J. M., Bremer, M. A. R., Huang, J. S., & Trentham, N. A. 1996, *ApJS*, 106, 215  
 Cimatti, A., Dey, A., van Breugel, W., Antonucci, R. & Spinrad, H. 1996, *ApJ*, 465, 145  
 De Young, D. S. 1989, *ApJ*, 342, L59  
 Evans, A. S. 1998, *ApJ*, 498, 553  
 Fabian, A. 1991, *MNRAS*, 238, 41  
 Graham, J. R., Carico, D. P., Matthews, K., Neugebauer, G., Soifer, B. T. & Wilson, T. D. 1990, *ApJ*, 354, L5  
 Kennicutt, R. 1983, *ApJ*, 272, 54  
 McCarthy, P. J., Persson, S. E., & West, S. C. 1992 *ApJ*, 386, 52  
 McCarthy, P. J., Kapahi, V., van Breugel, W. & Subrahmanya, C. 1990, *AJ*, 100, 1014  
 McIntosh, D. H., Rieke, M. J., Rix, H.-W., Foltz, C. B. & Weymann, R. J. 1999, *ApJ*, 514, 40  
 McLean, I. S., et al. 1998, *SPIE*, 3354, 566  
 McLean, I. S., et al. 2000, *PASP*, in preparation  
 Osterbrock, D.E. 1989, *Astrophysics of Gaseous Nebulae and Active Galactic Nuclei* (Mill Valley: University Science Books)  
 Pentericci, L., Rottgering, H. J., A., Miley, G. K., McCarthy, P., Spinrad, H., van Breugel, W. J. M., & Macchetto, F. 1999, *A&A*, 341, 329  
 Pettini, M., Kellogg, M. Steidel, C. C., Dickinson, M., Adelberger, K. L. & Giavalisco, M. 1998, *ApJ*, 508, 539  
 Rees, M. J. 1989, *MNRAS*, 239, 1  
 Teplitz, H. I. 2000, *ApJ*, submitted  
 van Breugel, W. J. M., Stanford, S. A., Spinrad, H., Stern, D., & Graham, J. R. 1998, *ApJ*, 502, 614  
 Villar-Martin, M., Binette, L. & Fosbury, R. A. E. 1999a, 346, 7  
 Villar-Martin, M., Fosbury, R. A. E., Binette, L., Tadhunter, C. N., & Rocca-Volmerange, B. 1999b, accepted for *A&A*